Institute for Numerical Methods in Engineering

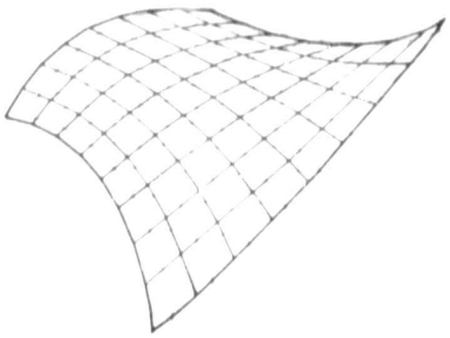

University College of Swansea, Singleton Park, Swansea, Wales, U.K. SA2 8PP. Telephone 0792 205678

HIGH SPEED INVISCID COMPRESSIBLE FLOW BY THE FINITE ELEMENT METHOD

O. C. Zienkiewicz, R. Löhner & K. Morgan

C/R/477/84 May 1984

Paper presented at the 5th MAFELAP Conference, Brunel University, 1-4 May, 1984.

HIGH SPEED INVISCID COMPRESSIBLE FLOW BY THE FINITE ELEMENT METHOD

O.C.Zienkiewicz, R.Löhner and K.Morgan

University of Wales, Swansea, Great Britain

1. INTRODUCTION

The numerical solution of compressible flow problems has received much attention over the past thiry years due, to a large extent, to the interests of the aerospace industry. The solutions of such problems are characterised by the appearance of discontinuities,such as shock waves, in the flow field and a major topic of attention has been the deveopment of numerical techniques which are able to adequately resolve such phenomena. A recent paper by Woodward and Collella [1] gives an excellent survey of the existing 'state of the art' and compares the performance of various widely used algorithms for certain test problems. The algorithms considered are finite difference/finite volume based and utilise either artificial viscosity [2], linear hybridization [3] or explicit nonlinearity [4]. All the schemes considered are shown to possess certain advantages and disadvantages.

The finite element method has only recently made its appearance in this area, but it is expected that it will make a significant contribution because of the great geometrical flexibility which is inherent in the method. A recent paper by Hughes [5] investigates the approach of explicit nonlinearity in a finite element context. The present authors have made some initial studies [6-8] of high speed inviscid flow problems in which they have used the finite element method and an explicit time stepping algorithm which is based on the Taylor-Galerkin schemes of Donea et al [9-12], with an appropriate artificial viscosity [13]. In this paper, we combine this solution algorithm with an automatic mesh refinement process which is designed to produce accurate steady state solutions to problems of inviscid compressible flow in two dimensions. The results of two test problems are included which demonstrate the excellent performance characteristics of the proposed procedures.

2. A SINGLE STEP ALGORITHM.

Inviscid compressible flow of an ideal gas in two dimensions is governed by the Euler equations, which can be written in vector form as

$$\frac{\partial \underline{U}}{\partial t} + \frac{\partial \underline{F}_j}{\partial x_j} = \underline{0} \qquad j=1,2 \tag{2.1}$$

where

$$\underline{U} = \begin{bmatrix} \rho \\ \rho u_1 \\ \rho u_2 \\ \rho e \end{bmatrix} \qquad \underline{F}_j = \begin{bmatrix} \rho u_j \\ \rho u_1 u_j + p\,\delta_{j1} \\ \rho u_2 u_j + p\,\delta_{j2} \\ u_j(\rho e + p) \end{bmatrix} \tag{2.2}$$

together with an equation of state

$$p = (\gamma-1)\rho\left[e - \tfrac{1}{2} u_j u_j\right] \tag{2.3}$$

Here p, ρ and e denote the pressure, density and specific internally energy of the fluid respectively while u_j is the velocity component in direction x_j of a Cartesian coordinate system. In addition, the summation convention is employed with δ_{ij} denoting the Kronecker delta.

A single step algorithm for the solutiion of (2.1) has been fully described elsewhere [6] and is based upon the Taylor-Galerkin methods of Donea et al [9-12]. A brief descripion of the solution procedure will be given here for the sake of completeness.

Using a Taylor series expansion about time $t = t^n$ gives

$$\underline{U}^{n+1} = \underline{U}^n + \Delta t \left.\frac{\partial \underline{U}}{\partial t}\right|^n + \left.\frac{\Delta t^2}{2}\frac{\partial^2 \underline{U}}{\partial t^2}\right|^n \tag{2.4}$$

correct to second order, where $t^{n+1} = t^n + \Delta t$ and a superscript n denotes an evaluation at time $t = t^n$. Eliminating the time derivatives via (2.1) leads to the time-stepping scheme

$$\underline{U}^{n+1} = \underline{U}^n - \Delta t \left.\frac{\partial \underline{F}_j}{\partial x_j}\right|^n + \left.\frac{\Delta t^2}{2}\frac{\partial}{\partial x_k}\left[\underline{A}_k \frac{\partial \underline{F}_j}{\partial x_j}\right]\right|^n \tag{2.5}$$

where

$$\underline{A}_k = \frac{\partial \underline{F}_k}{\partial \underline{U}} \tag{2.6}$$

The region $\mathcal{R}$ over which the solution is required is discretised using linear 3-noded triangular elements and a Galerkin finite element solution procedure is applied to (2.5) using approximations

$$\underline{U} \approx \underline{U}^* = \sum_m \underline{U}_m N_m$$

$$\underline{F}_j \approx \underline{F}_j^* = \sum_m \underline{F}_{jm} N_m \qquad (2.7)$$

$$\underline{A}_k \approx \underline{A}_k^* = \sum_e \underline{A}_{ke} P_e$$

Here N_m denotes the piecewise linear shape function associated with node m and P_e the piecewise constant shape function associated with element e. The resulting matrix equation system takes the form

$$\underline{M}(\hat{\underline{U}}^{n+1} - \hat{\underline{U}}^n) = \underline{f}^n \qquad (2.8)$$

where

$$\hat{\underline{U}}^T = (\underline{U}_1, \underline{U}_2, \ldots\ldots) \qquad (2.9)$$

and $\underline{M}$ is a standard mass matrix. An explicit solution procedure for (2.8) is adopted. For problems involving strong shocks an artificial viscosity term is included. The form used is due to Lapidus [13] and replaces the quantities calculated from (2.8) by smoothed values

$$\underline{U}_{ms}^{n+1} = \underline{U}_m^{n+1} - C_\nu \Delta t \sum_{j,e} h_e^2 \int_{\mathcal{R}_e} \left| \frac{\partial \underline{u}_j}{\partial x_j} \right| \frac{\partial \underline{U}^{n+1}}{\partial x_j} \frac{\partial N_m}{\partial x_j} d\mathcal{R} \qquad (2.10)$$

where C_ν is a constant in the range $0.5 \leq C_\nu \leq 2$ and h_e^2 is a representative area for element e.

3 A TWO STEP ALGORITHM

Finite difference workers have consistently avoided the use of single step explicit algorithms because of the computational expense involved in performing matrix multiplications of the form required in (2.5). They have favoured instead two-step methods which are designed to avoid this requirement. A finite element two-step algorithm may be produced which has certain features in common with the finite difference scheme of Burstein [14]. Alternative finite element two step algorithm has recently been proposed by Miner and Skop [15].

3.1 The First Step

Using a Taylor series expansion about time $t=t^n$ gives

$$\underline{U}^{n+\alpha} = \underline{U}^n + \alpha \Delta t \left.\frac{\partial \underline{U}}{\partial t}\right|^n \tag{3.1}$$

correct to first order, where $t^{n+\alpha} = t^n + \alpha\Delta t$, and replacing the time derivative from (2.1) produces the expression

$$\underline{U}^{n+\alpha} = \underline{U}^n - \alpha \Delta t \left.\frac{\partial \underline{F}_j}{\partial x_j}\right|^n \tag{3.2}$$

Employing triangular elements with piecewise linear and piecewise constant shape functions as previously defined, approximations are taken in the form.

$$\begin{aligned} \underline{U}^n &\approx \underline{U}^{*n} = \sum_m \underline{U}^n_m N_m \\ \underline{U}^{n+\alpha} &\approx \underline{U}^{*n+\alpha} = \sum_e \underline{U}_e^{n+\alpha} P_e \\ \underline{F}_j^n &\approx \underline{F}_j^{*n} = \sum_m \underline{F}_{jm}^n N_m \end{aligned} \tag{3.3}$$

These approximations are substituted into (3.2) and a weighted residual statement [16] is formed using the weighting function P_E. The result is to give $\underline{U}_E^{n+\alpha}$ immediately as

$$\Delta_E \underline{U}_E^{n+\alpha} = \sum_m \underline{U}_m^n \int_{\Omega_E} N_m d\Omega - \alpha\Delta t \sum_m \underline{F}_{jm}^n \int_{\Omega_E} \frac{\partial N_m}{\partial x_j} d\Omega \tag{3.4}$$

where Δ_E denotes the area of element E and Ω_E denotes the surface of this element. It may be observed that $\underline{U}_E^{n+\alpha}$ can be obtained quickly as no assembly of element conributions is required to form the right hand side of (3.4).

3.2 The Second Step

The second step begins by making a new Taylor expansion and writing

$$\underline{U}^{n+1} = \underline{U}^n + \Delta t \left.\frac{\partial \underline{U}}{\partial t}\right|^{n+\alpha} \tag{3.5}$$

and again replacing the time derivative leads to

$$\underline{U}^{n+1} = \underline{U}^n - \Delta t \left.\frac{\partial \underline{F}_j}{\partial x_j}\right|^{n+\alpha} \tag{3.6}$$

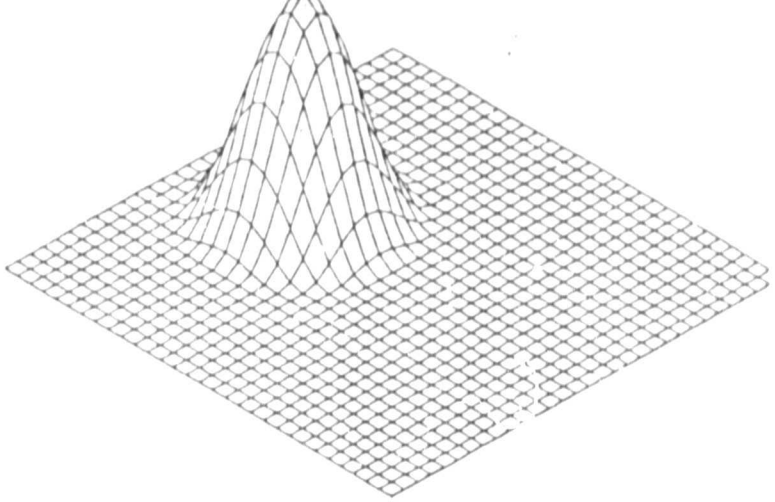

(a)

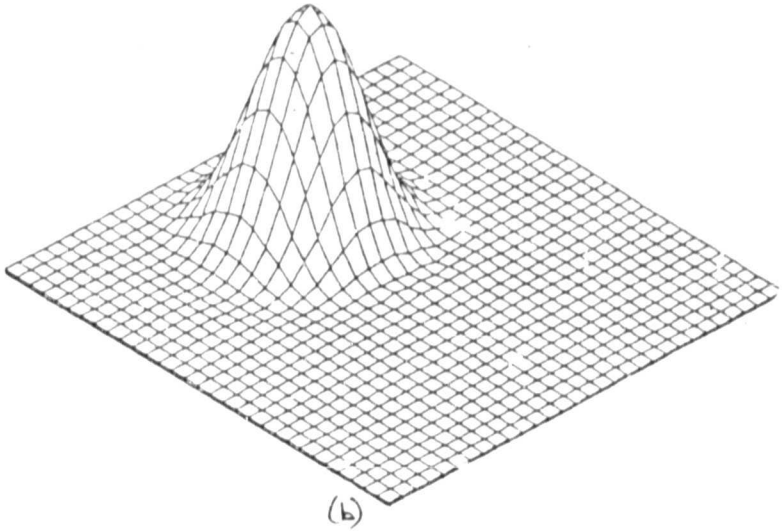

(b)

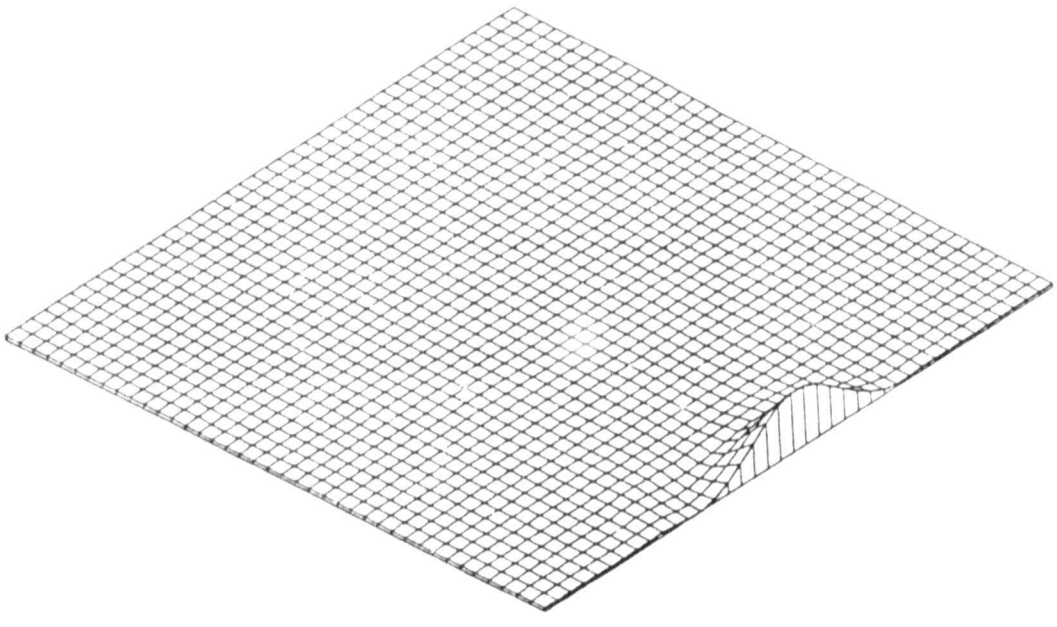

(c)

FIG. 1. Pure advection in two dimensions. (a) Initial concentration profile (b) Profile after one complete revolution in a rotating velocity field (c) Profile about to leave the region in an uniform velocity field

With the approximations

$$\underline{U}^{n+1} \approx \underline{U}^{*\,n+1} = \sum_m \underline{U}_m^{n+1} N_m$$
$$\underline{F}_j^{n+\alpha} \approx \underline{F}_j^{*\,n+\alpha} = \sum_e \underline{F}_{je}^{n+\alpha} P_e \qquad (3.7)$$

an appropriated wieghted residual form for (3.6) is then

$$\int_\Omega \underline{U}^{n+1} N_\ell \, d\Omega = \int_\Omega \underline{U}^n N_\ell \, d\Omega + \Delta t \int_\Omega \underline{F}_j^{n+\alpha} \frac{\partial N_\ell}{\partial x_j} d\Omega - \Delta t \int_\Gamma \ell_j \underline{F}_j^{n+\alpha} N_\ell \, d\Gamma \qquad (3.8)$$

where $\underline{n} = (\ell_1, \ell_2)$ is the unit outward normal to the boundary Γ of Ω. Inserting (3.7) into (3.8) then gives

$$\underline{M}\,(\hat{\underline{U}}^{n+1} - \hat{\underline{U}}^n) = \underline{q}^{n+\alpha} \qquad (3.9)$$

where $\hat{\underline{U}}$ is defined in (2.9). The solution of this equation completes the second step. Again the smoothing of (2.10) is applied for problems involving strong shocks. It should be noted that for linear problems where

$$\underline{F}_k = \underline{A}_k \underline{U} \qquad (3.10)$$

and $\underline{A}_k$ is constant, (3.8) combined with (3.9) produces exactly the single step equation system (2.8) when $\alpha = 1/2$.

This has been confirmed computationally by applying both methods to the solution of pure advection problems involving a cone-shaped profile in two dimensions. Similar problems have been studied extensively in recent years [9, 17, 18].For this problem, the governing equation is the scalar equation.

$$\frac{\partial U}{\partial t} + A_k \frac{\partial U}{\partial x_k} = 0 \qquad (3.11)$$

where (A_1, A_2) denotes a specified velocity field and U denotes the concentration. Fig.1a shows the initial profile and Fig.1b illustrates the numerical solution produced after one complete rotation in an incompressible rotating velocity field. A problem involving the transportation out of the domain of interest of an initial cone in an uniform velocity field was also investigated. Fig.1c shows the profile of the concentration as the cone is about to leave the region completely. The quality of these results is excellent and they

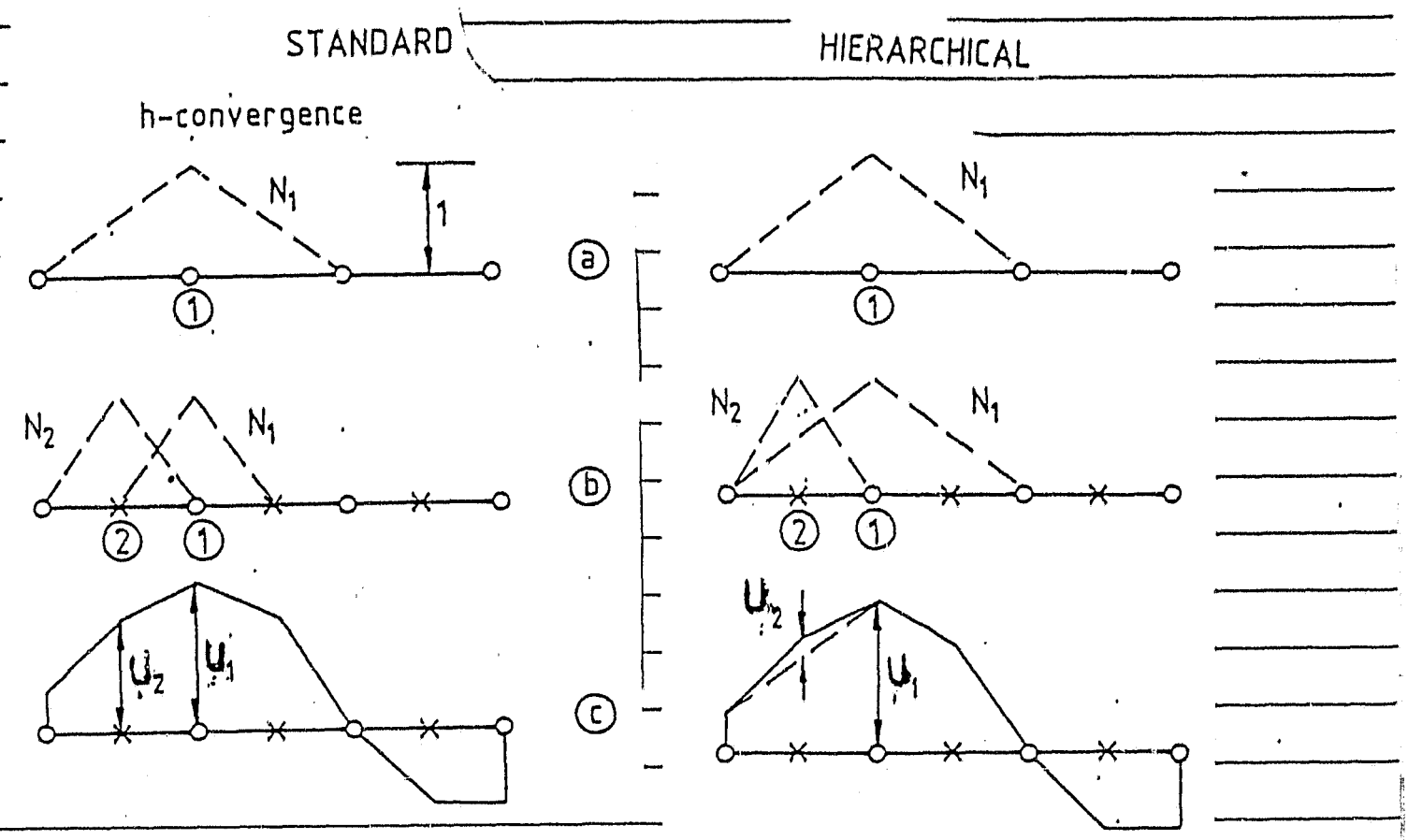

FIG.2. Comparison between standard and hierarchical refinement processes. (a) Original mesh (b) Refined mesh (c) Approximation to a function $u \approx \sum_j u_j N_j$

were produced without the artificial viscosity term of (2.10) i.e. $C_\mu = 0$.

Preliminary tests show the single step and two step algorithms to be producing similar results for practical problems involving the non-linear equation set (2.1) - (2.3), with the two step method proving to be computationally more efficient.

4. DOMAIN SPLITTING

It is well-known that solutions of high speed inviscid compressible flow problems exhibit narrow regions of rapid change (e.g.shocks) which are embedded in larger regions where the solution is smooth. The economical method of producing an accurate solution is to use a discretisation which has many small elements in the region of rapid change and larger elements elsewhere. However, the small elements used might then require that a correspondingly small value of the timestep, t, has to be employed to ensure stability of the algorithms described in the previous section, whereas the larger elements could tolerate the use of a bigger timestep. The remedy adopted by the authors is to split the domain into regions in which different timestep sizes can be used. This method, which bears certain resemblances to the explicit-explicit procedures of Belytschko et al [19] and Liu [20] is described in detail elsewhere [7] and will not be considered further here. It should be noted however that this procedure is performed completely automatically by the computer code at prescribed times during the analysis.

5. ADAPTIVE MESH REFINEMENT

In general, an analyst will have no a priori knowledge of the location of those areas of the solution domain in which large gradients will exist. An ideal computational algorithm would then require the ability to automatically refine the finite element mesh, in zones of high gradients, as the computation proceeds. The geometric flexibility of the linear triangular element makes it ideally suited to refinement processes of this type.

Adaptive refinement techniques are currently receiving much attention [21,22] and two general classes may be identified.viz a priori methods and a posteriori methods. Although many applications employing a priori grid refinements have been reported, at the present time this approach appears to compare unfavourably with a posteriori methods with regard to CPU time requirements [21]. For this reason, we have concentrated on the use of a posteriori techniques. Here the solution is

obtained on an original mesh and, at a certain time, the mesh is refined according to some strategy. The solution then proceeds, with further refinements being made as required. The authors have investigated two alternative refinement stategies viz mesh movement and mesh enrichment.

5.1 Mesh Movement

Here the total number of nodes and elements remains constant, but the location of the nodes is changes in order to achieve a better overall distribution. Full details of the strategy adopted for moving the mesh and handling some of the subsequent problems which may arise have been given in detail elsewhere [8]. This approach alone does not appear to possess the degree of flexibility which would be required for general aerodynamic problems and so it has been replaced by mesh enrichment.

5.2 Mesh Enrichment

In this case the original mesh is held fixed, while hierarchical elements [16] or simply more elements are added. Both strategies have their merits and disadvantages. If further degrees of freedom are added hierarchicially, the old shape functions are trained and the new shape functions are retained and the new shape functions are introduced for relative values of the unknown. Fig.2 shows the comparison of this strategy with the classical enrichment method of adding more elements. The advetages of the herarchical technique are (i) certain matrices may be re-used, so avoiding some recomputation (ii) multigrid solvers may be implemented naturally (iii) no geometrical problems are encountered in the transition zone between refined and unrefined portions of the mesh. The disadvantages of the hierarchical approach are (i) more stiffness coefficients appear as all the refinement levels are interconnected (ii) the program structure becomes very involved and, it is expected that, efficient vectorisation will be virtually impossible.

The classical way of enriching grids is simply to add more elements. In this case, all the advantages of the hierarchical method are lost whle the disadvantages disappear. However, when a detailed comparison was made of the two possibilities [23], it was decided that classical enrichment would be more efficient at this stage for general transient problems and so this method was implemented in the computer code.

5.3 Error Estimate

Consider a single scalar equation with unknown U and a

corresponding finite element approximation U*. The aim of any adaptive mesh refinement is to attempt to minimise the highest error occurring in the elements representing the domain i.e.

$$\epsilon = \max_{e} \| U - U^* \|_k^e \qquad (5.1)$$

should be minimised, where $\| \quad \|_k$ denotes some suitable norm. This criterion leads to the requirement that the error should be evenly distributed across the domain, which amounts to the requirement

$$\| U - U^* \|_k^e = \text{constant} \qquad (5.2)$$

For elliptic problems, the appropriate norm appears naturally as the energy norm and a fairly complete and general theory of error estimators is available [24,25]. However, far less research has been directed towards hyperbolic problems and a detailed theory is still lacking. Here we attempt to derive a simple, yet reliable, error criterion for hyperbolic problems and linear elements.

It has been shown by Strang and Fix [26] that a natural norm for first order hyperbolic equations is the L_2 defined by

$$\| V \|_0^e = \left\{ \int_{\Omega_e} |V|^2 \, d\Omega \right\}^{1/2} \qquad (5.3)$$

If the solution of hyperbolic equations is viewed as an approximation problem along characteristics then it can be shown [26] that

$$\| U - U^* \|_k^e \leq K h_e^{l-k} \| U \|_l^e \qquad (5.4)$$

where h_e is a representative element legnth, and using the L_2 norm of (5.3) gives

$$\| U - U^* \|_0^e \leq K h_e^{l} \| U \|_l^e \qquad (5.5)$$

The condition of (5.2) is then replaced by the requirement that

$$h_e^l \| U \|_l^e = \text{constant} \qquad (5.6)$$

or, since the exact solution U is unknown, the practical requirement becomes

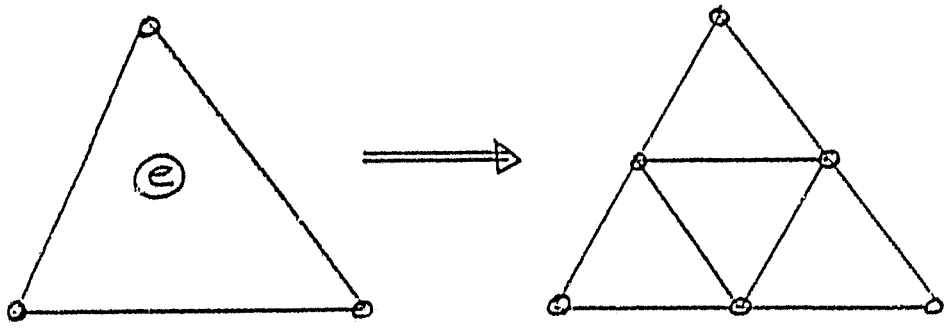

(a)

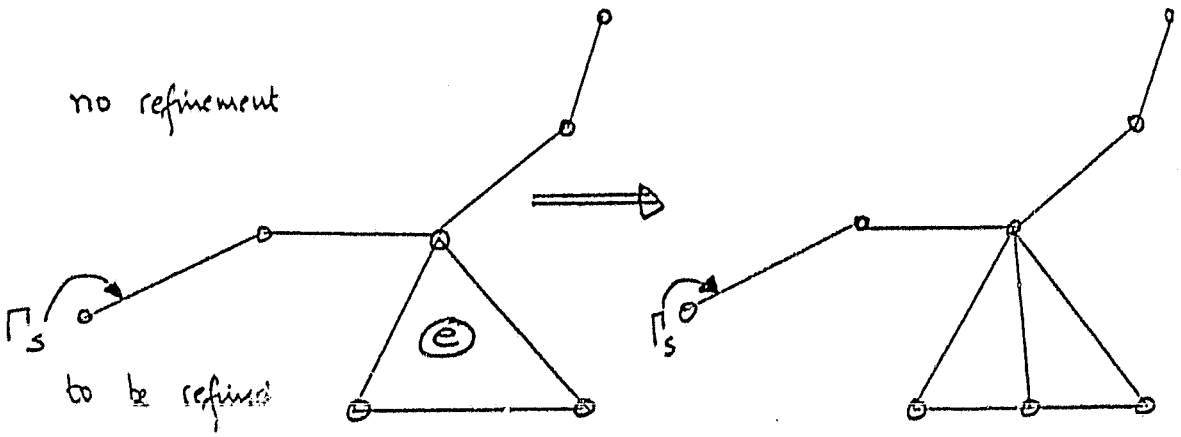

(b)

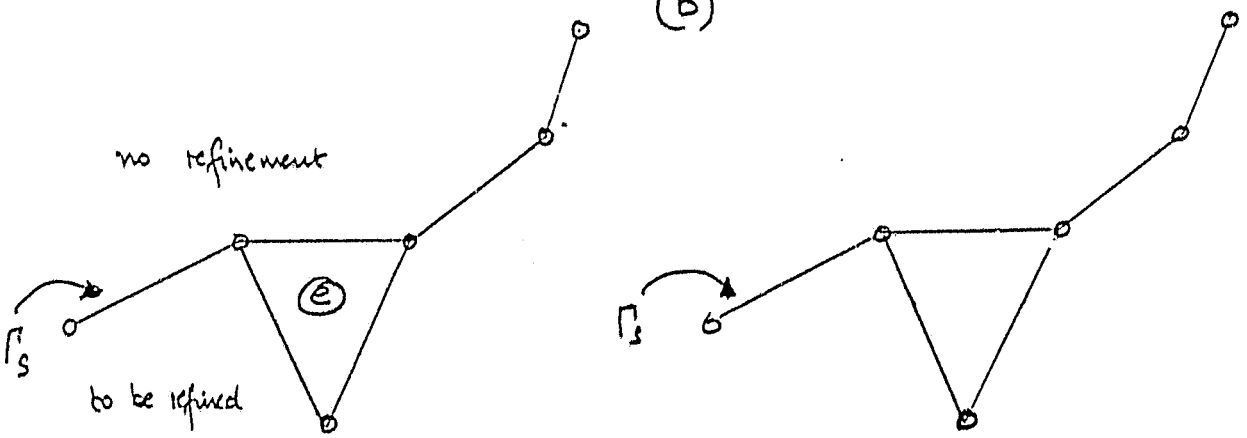

(c)

FIG. 3 The refinement of element e. (a) No nodes on Γ_s (b) one node on Γ_s (c) two nodes on Γ_s.

$$h_e^{\ell} \, \| U^* \|_{\ell}^{e} = \text{constant} \qquad (5.7)$$

If linear elements are being employed it seems natural to choose $\ell = 1$ and to define

$$\| U^* \|_1^e = \left\{ \int_{\Omega_e} \left(\frac{\partial U^*}{\partial x_i} \right)^2 d\Omega \right\}^{1/2} \qquad (5.8)$$

If the elements are not badly deformed then (5.7) may be approximated by the requirement that

$$\Psi^e = h_e^{\beta} \left\{ \max_e U^* - \min_e U^* \right\} = \text{constant} \qquad (5.9)$$

where $\beta = 1/2$, 1 or $3/2$ for one, two or three dimensions respectively.

5.4 Identification of Regions to be Refined.

The first step in any mesh refinement algorithm is the identification of the regions of the domain in which refinement is to be employed. For (5.9) it is clear that all elements which satisfy

$$\Psi^e > \delta \max_e \Psi^e \qquad (5.10)$$

should be refined further. The constant δ in this equation acts as a threshold value for the refinement process. Having identified in this fashion the patches of elements that are to be refined, the boundary nodes of these patches are obtained. In order to avoid 'saw-tooth' type boundary shapes, any element which has all its node on these boundaries is itself included among the list of elements to be refined.

For systems of equations, a 'key-variable' has to be identified in order to employ (5.10). The choice of this variable is not obvious but the density has been chosen for the computations reported here.

5.5 Subdivision of the Elements.

During the subdivision process, three different types of element can appear according to the number of nodes of the element which lie on the boundary Γ_s between the region which is to be subdivided and the region which is to remain

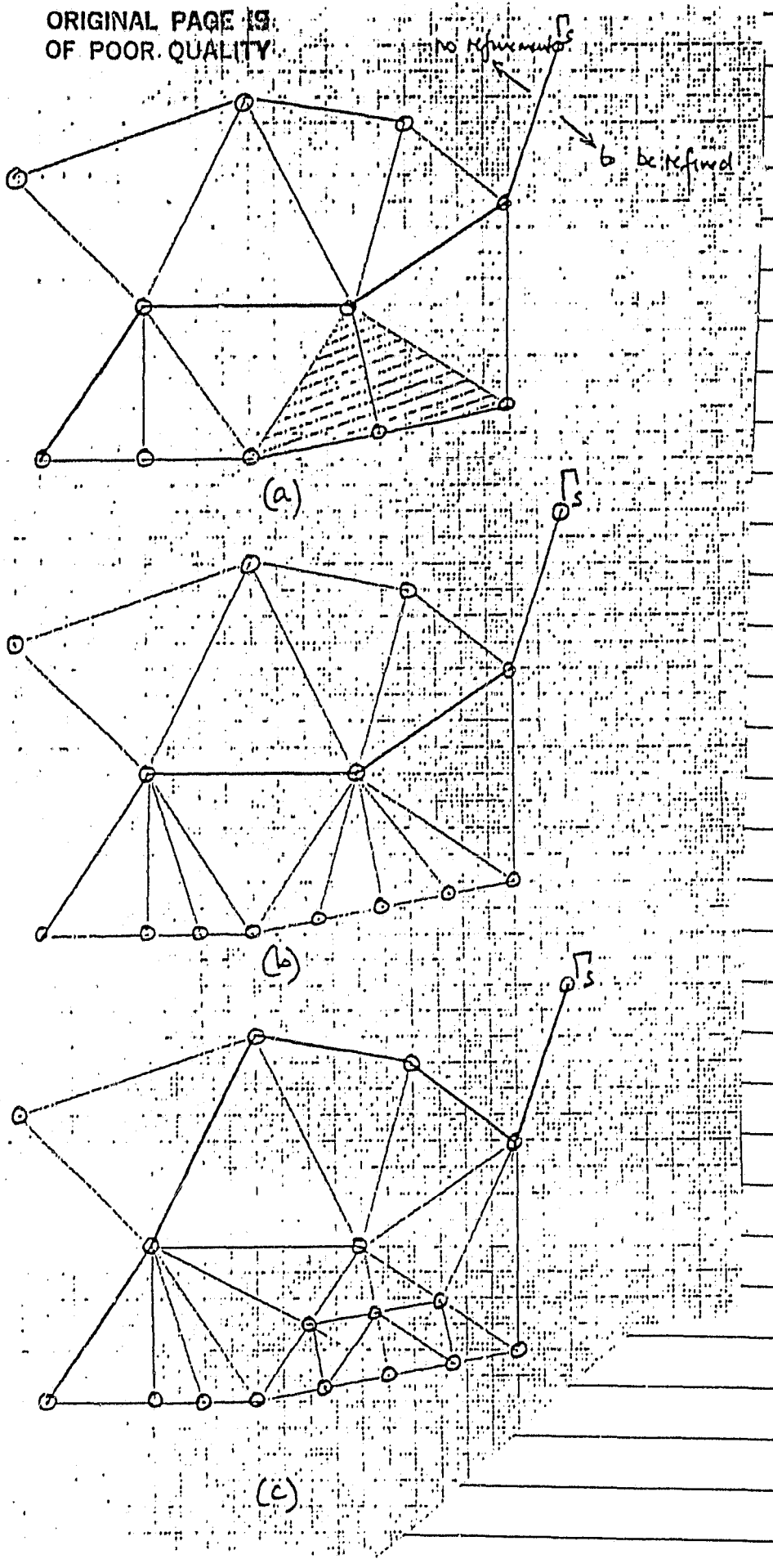

FIG. 4. Avoidance of successive subdivision into two during refinement
(a) The shaded element has already been subdivided at a previous step.
(b) This scheme is not adopted (c) This is the adopted scheme.

unchanged. If the element has no nodes on Γ_S then the element is simply divided into four elements as shown in Fig.3a. If the element has one node on Γ_S then the element is subdivided into two elements as shown in Fig.3b. Finally, if the element has more than one node on Γ_S then no subdivision is performed as shown in Fig.3c. When this process has been carried out, the new nodal coordinates and the new nodal unknowns are calculated while the new element connectivites are formed. The subdivision process is completed by identifying new nodes which lie on the boundary of the physical domain and assigning to these nodes the appropriate boundary condition marker.

5.6 Mesh Quality Enhancement

In many practical situations the straightforward subdivision strategy described above will prove satisfactory but, under certain circumstances, badly deformed elements can appear. Three simple devices hve thus been implemented in an attempt to improve the quality of the refined mesh and these are described below. The resulting meshes are generally free of the geometrical difficulties usually encountered when meshes are enriched by straightforward subdivision. In addition, these strategies can easily be extended to three dimensions if linear tetrahedral elements are employed.

5.6.1 Smoothing With the refined grid, the sides of the elements are replaced by springs of unit stiffness. For badly deformed elements the resulting nodal forces will not be in equilibrium, whereas for regions of well-formed elements the resulting nodal forces will nearly vanish. A relaxation procedure [8] is adopted which moves the nodes until equilibrium of the nodal forces is achieved. Five steps of this process are normally employed and this ensures a local smoothing of the mesh.

5.6.2 Avoidance of Successive Subdivision into Two Badly deformed elements can appear when an element that has been initially divided into two elements as in Fig.3b is again subdivided in the same fashion. The easiest method of avoiding this second subdivision is to enlarge the region which is to be refined by adding to it all elements surrounding the element under consideration. The element under consideration can then be subdivided into eight elements, thus enhancing the regularity of the mesh. This process is illustrated in Fig.4.

5.6.3 Removal of Badly Deformed Elements If badly deformed elements are still present, after avoiding successive

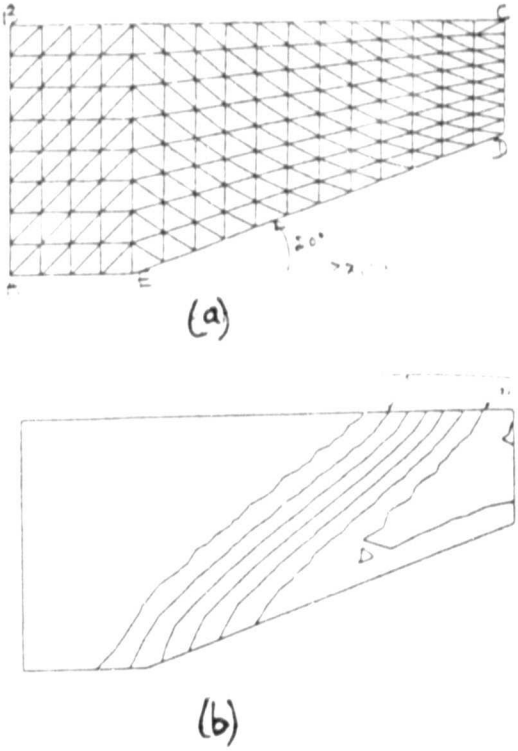

FIG. 5. Supersonic flow past a wedge at Mach 2. (a) Initial mesh (b) Density after 100 steps.

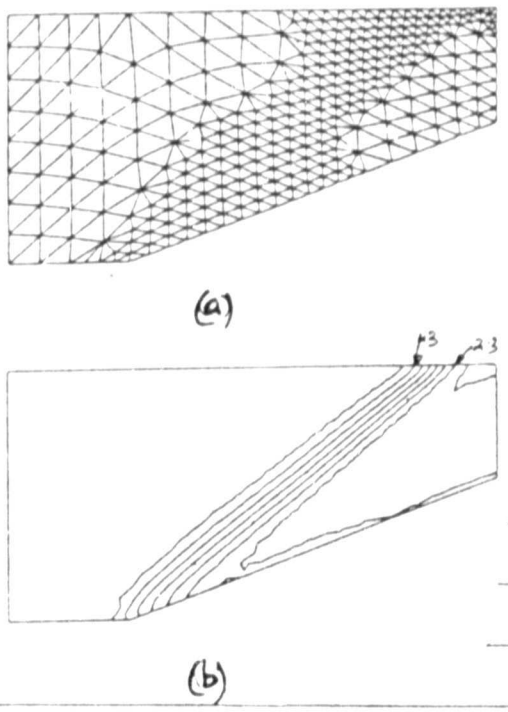

FIG. 6. Supersonic flow past a wedge at Mach 2. (a) First mesh refinement (b) Density after a further 100 time steps.

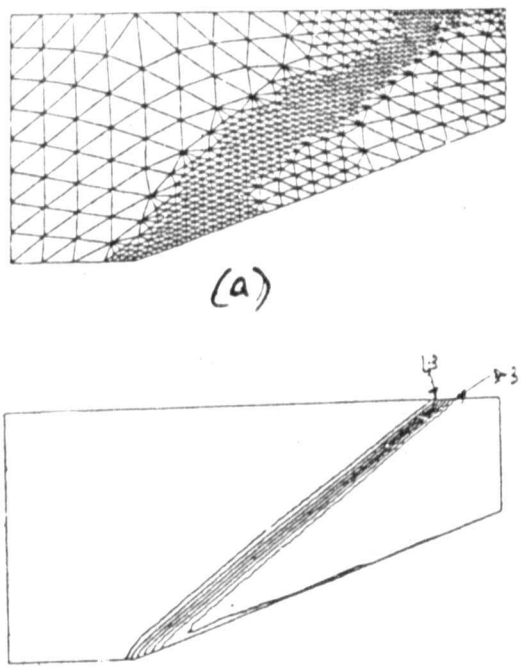

FIG. 7. Supersonic flow past a wedge at Mach 2. (a) Second mesh refinement
(b) Density after a further 100 global time steps.

subdivision into two and after smoothing the mesh, then these elements are removed from the computation. This algorithm is detailed elsewhere [8] and need not be repeated here.

6. RESULTS

Results will be presented which show the application of the methods described in this paper to two separate problems viz. steady supersonic flow past a wedge and steady supersonic flow past a nose cone. As both problems are steady, the transient algorithms described previously are used here as a device for integrating to steady state.

6.1 Supersonic Flow Past a Wedge

The solution domain and the initial discretisation is shown in Fig.5a. Along AB the flow variables are held fixed at the values $\rho = 1.125$, $u_1 = 1020$, $u_2 = 0$, $e = 727350$ giving a free stream Mach number of three. The boundary ED is a solid wall while 'natural' conditions are applied along BC, CD and AE. The exact solution for this problem consists of an attached plane shock at an angle of 37.5° to the x_1-axis with uniform flow ahead of and behind the shock.

The density distribution after 100 global timesteps is shown in Fig.5b, and, although the required features are present, the quality of the solution is not good because of the coarseness of the initial discretisation. The mesh is therefore automatically refined at this stage, as shown in Fig.6a, and the solution is advanced in time. After a further 100 global steps the density distribution is as illustrated in Fig.6b and the improvement in the quality of the solution is apparent. A further refinement was performed, producing the mesh of Fig.7a, whch produced the density distribution shown in Fig.7b after a further 100 global steps. The quality of this solution is excellent when compared with the behaviour of the exact solution.

6.2 Supersonic Flow Past a Nose Cone

The solution domain and initial discretisation for this example is shown in Fig.8. Along AB the flow variables are held fixed at the values $\rho = 1$, $u_1 = 1.028$, $u_2 = 0$, $e = 1$ giving a free stream Mach number of two. The boundary CD is a solid wall and 'natural' conditions are applied over BC and DA. The initial finite element discretisation is shown in Fig.8 and the solution was advanced 100 global timesteps on this mesh. The mesh was then refined as shown in Fig.9a and after a further 100 global time steps the density distribution is as illustrated in Fig.9b. The next level of refinement is

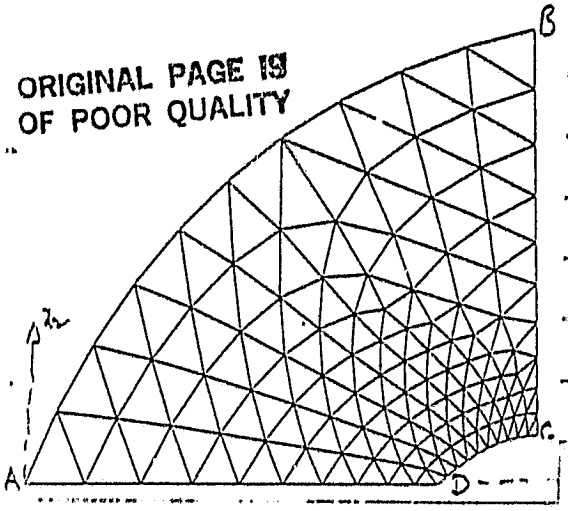

FIG. 8. Supersonic flow past a nose cone — initial mesh.

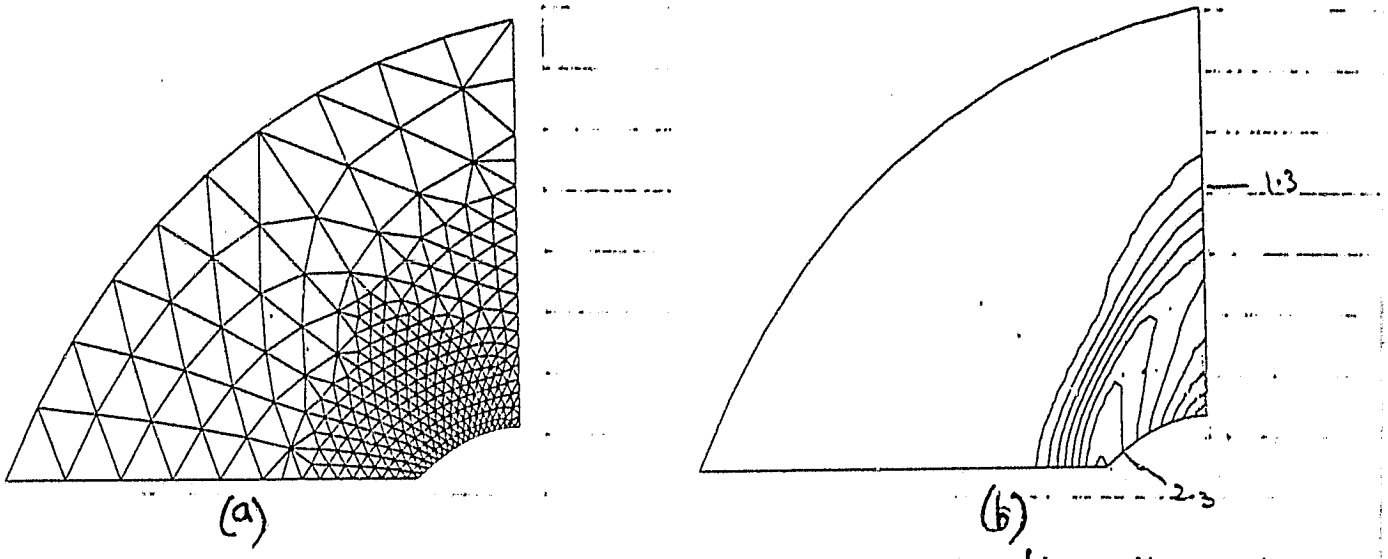

(a) (b)

FIG. 9. Supersonic flow past a nose cone (a) First mesh refinement after 100 global time steps (b) Density distribution after a further 100 global time steps.

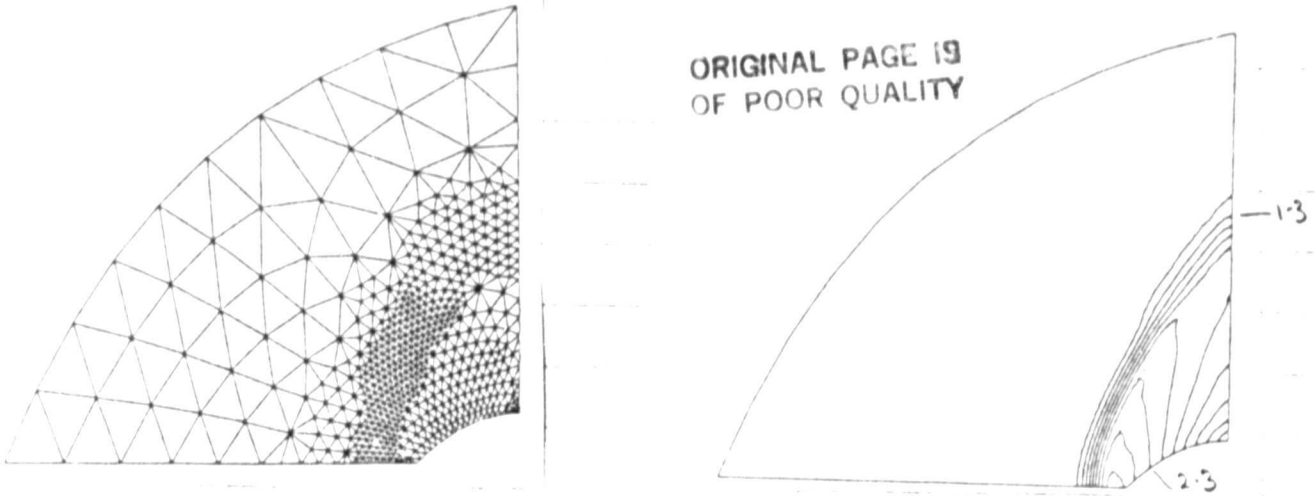

(a) (b)

FIG.10. Supersonic flow past a nose cone (a) Second mesh refinement (b) Density distribution after a further 100 global time steps.

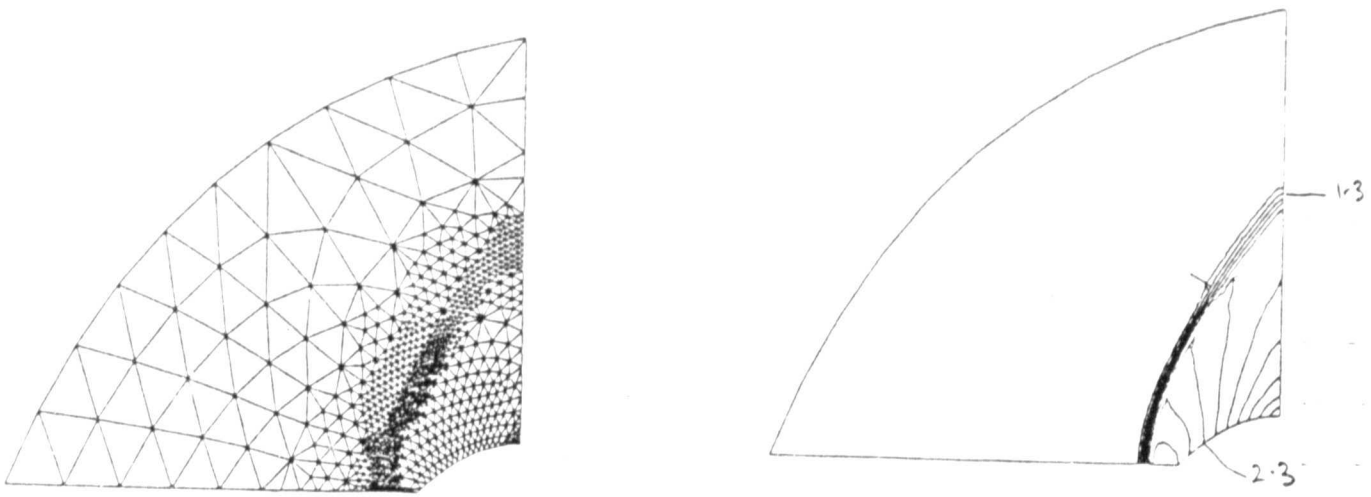

(a) (b)

FIG.11. Supersonic flow past a nose cone (a) Final mesh (b) Density distribution after a further 20 global time steps.

displayed in Fig.10a with the corresponding density contours after a further 100 global steps appearing in Fig.10b. The final refinement is then performed as in Fig.11a, producing the density contours of Fig.11b after a further 10 global time steps. The quality of the final solution is good, showing the detached bow shock.

7. CONCLUSIONS

Explicit solution techniques for the Euler equations have been combined with domain splitting and mesh enrichment procedures. Practical examples have been presented which confirm the viability of the procedures for the analysis of steady problems. For the analysis of true transient problems, the areas requiring refinement will traverse the whole of the domain under consideration and the refinement strategy will require suitable modification in this case [23].

8. ACNOWLEDGEMENT

The authors would like to thank the Aerothermal Loads Branch, NASA Langley Research Center for supporting this research under Grant No. NAGW-478, and especially A.R.Wieting and K.S.Bey for guidance and encouragement.

9. REFERENCES

1. WOODWARD, P. and COLELLA, P, 'The numerical solution of 2D fluid flow with strong shocks' **J.Comp.Phys.** (1984, to appear).

2. VON NEUMANN, J. and RICHTMEYER, R.D., 'A method for the numerical calculation of hydrodynamic shocks', **J.Appl.Phys.**21, 232-236 (1950)

3. HARTEN, A. and ZWAS, G., 'Self-adjusting hybrid schemes for shock computations', **J.Comp.Phys.**6,568-583 (1972)

4. GODUNOV, S.K., 'Finite difference methods for numerical computations of discontinuous solutions of equations of fluid dynamics', Mat.Sb., 47, 271-295 (1959)

5. HUGHES, T.J.R., 'A shock-capturing finite element method'. Preprint (1984).

6. LOHNER, R., MORGAN, K. and ZIENKIEWICZ, O.C., 'The solution of non-linear systems of hyperbolic equations by the finite element method', accepted for publication **Int.J.Num.Meth.Fluids** (1984).

7. LOHNER, R., MORGAN, K. and ZIENKIEWICZ, O.C., 'The use of domain splitting with an explicit hyperbolic solver', accepted for publication in **Comp.Meth.Appl.Mech.Engng.** (1984).

8. LOHNER, R., MORGAN, K. and ZIENKIEWICZ, O.C., 'Adaptive grid refinement for the Euler and compressible Navier-Stokes equations', to appear in **Proc.Conf.Accuracy** Estimates and Adaptive Refinements in Finite Element Computations Lisbon (1984).

9. DONEA, J., 'A Taylor-Galerkin method for convective transport problems', **Int.J.Num.Meth.Engg.** 20, 101-120 (1984).

10. DONEA, J., GIULIANI, S., LAVAL, H. and QUARTAPELLE, L., 'Time accurate solution of advection-diffusion problems by finite elements', accepted for publication in **Comp.Meth.Appl.Mech.Engg.** (1984).

11. DONEA, J., 'Recent advances in computational methods for steady and transient transport problems', accepted for publication in **Nucl.Engng.Des.** (1984).

12. SELMIN, V., DONEA, J. and QUARTAPELLE, L., 'Taylor-Galerkin method for non-linear hyperbolic equations', to appear in **Proc.Conf.Numerical Methods for Transient and Coupled Problems**, Venice (1984).

13. LAPIDUS, A., 'A detached shock calculation by second-order finite differences', **J.Comp.Phys.**, 2, 154-177 (1967).

14. BURSTEIN, S.Z., 'Finite difference calculations for hydrodynamic flows containing discontinuities', **J.Comp. Physc.**2, 198-222 (1967).

15. MINER, E.W. and SKOP, R.A., 'Explicit time integration for the finite element shock wave equations', AIAA Paper 82 - 0994 (1982).

16. ZIENKIEWICZ, O.C. and MORGAN, K., **'Finite elements and approximation'**, John Wiley, New York (1983).

17. HUGHES, T.J.R. and BROOKS, A., 'A multidimensionsal upwind scheme with no cross-wind diffusion', **ASME AMD**, 34, 19-36 (1979)

18. BAKER, A.J., **Finite element computational fluid mechanics'**, Hemisphere, Washington (1983).

19. BELYTSCHKO, T., YEN, H.I. and MULLEN, R.,'Mixed Methods for time integration', Comp.Meth.Appl.Mech.Engng.,17-18, 259-275 (1979)

20. LIU, W.K., 'Development of mixed time partition procedures for thermal analysis of structures', Int.J.Num.Meth.Engng.,19,125-140 (1983).

21. ODEN, J.T. 'Notes on grid optimization and adaptive methods for finite element methods', TICOM Report (1983).

22. THOMPSON, J.F. (Editor), 'Numerical grid generation', Elsevier, New York (1982).

23. LOHNER, R., Ph.D. Thesis, University of Wales (1984).

24. BABUSKA, I. and RHEINBOLDT, W.C., 'A-posteriori error estimates for the finite element method', Int.J.Num.Meth.Engng.,12, 1597-1615 (1978).

25. BABUSKA, I. and RHEINBOLDT, W.C., 'Computational error estimates and adaptive processes for some structural problems',Comp.Meth.Appl.Mech.Engng.34, 895-937 (1982).

26. STRANG, G. and FIX, G.J., 'An analysis of the finite element method' Prentice-Hall, Englewood Cliffs (1976).